

Microscopic spin Hamiltonian approaches for $3d^8$ and $3d^2$ ions in a trigonal crystal field - perturbation theory methods versus complete diagonalization methods

This article has been downloaded from IOPscience. Please scroll down to see the full text article.

2002 J. Phys.: Condens. Matter 14 5619

(<http://iopscience.iop.org/0953-8984/14/22/314>)

View [the table of contents for this issue](#), or go to the [journal homepage](#) for more

Download details:

IP Address: 171.66.16.104

The article was downloaded on 18/05/2010 at 06:46

Please note that [terms and conditions apply](#).

Microscopic spin Hamiltonian approaches for $3d^8$ and $3d^2$ ions in a trigonal crystal field—perturbation theory methods versus complete diagonalization methods

Czeslaw Rudowicz^{1,3}, Yau-yuen Yeung², Zi-Yuan Yang^{1,4} and Jian Qin¹

¹ Department of Physics and Materials Science, City University of Hong Kong, 83 Tat Chee Avenue, Kowloon, Hong Kong SAR, People's Republic of China

² Department of Science, The Hong Kong Institute of Education, 10 Lo Ping Road, Tai Po, New Territories, Hong Kong SAR, People's Republic of China

E-mail: APCESLAW@cityu.edu.hk

Received 27 March 2002, in final form 24 April 2002

Published 23 May 2002

Online at stacks.iop.org/JPhysCM/14/5619

Abstract

In this paper, we critically review the existing microscopic spin Hamiltonian (MSH) approaches, namely the complete diagonalization method (CDM) and the perturbation theory method (PTM), for $3d^8(3d^2)$ ions in a trigonal (C_{3v} , D_3 , D_{3d}) symmetry crystal field (CF). A new CDM is presented and a CFA/MSH computer package based on our crystal-field analysis (CFA) package for $3d^N$ ions is developed for numerical calculations. Our method takes into account the contribution to the SH parameters (D , g_{\parallel} and g_{\perp}) from all 45 CF states for $3d^8(3d^2)$ ions and is based on the complete diagonalization of the Hamiltonian including the electrostatic interactions, the CF terms (in the intermediate CF scheme) and the spin-orbit coupling. The CFA/MSH package enables us to study not only the CF energy levels and wavefunctions but also the SH parameters as functions of the CF parameters (B_{20} , B_{40} and B_{43} or alternatively Dq , v and v') for $3d^8(3d^2)$ ions in trigonal symmetry. Extensive comparative studies of other MSH approaches are carried out using the CFA/MSH package. *First*, we check the accuracy of the approximate PTM based on the 'quasi-fourth-order' perturbation formulae developed by Petrosyan and Mirzakhanyan (PM). The present investigations indicate that the PM formulae for the g -factors (g_{\parallel} and g_{\perp}) indeed work well, especially for the cases of small v and v' and large Dq , whereas the PM formula for the zero-field splitting (ZFS) exhibits serious shortcomings. Earlier criticism of the PM approach by Zhou *et al* (Zhou K W, Zhao S B, Wu P F and Xie J K 1990 *Phys. Status Solidi b* **162** 193) is then revisited. *Second*, we carry out an extensive

³ Author to whom any correspondence should be addressed.

⁴ On leave from: Institute of Applied Physics and Department of Physics, Baoji College of Arts and Science, Baoji 721007, People's Republic of China.

comparison of the results of the present CFA/MSH package and those of other CDMs based on the strong- and weak-CF schemes. The CF energy levels and the SH parameters for $3d^2$ and $3d^8$ ions at C_{3v} symmetry sites in several crystals are calculated and analysed. Our investigations reveal serious inconsistencies in the CDM results of Zhou *et al* and Li (Li Y 1995 *J. Phys.: Condens. Matter* **7** 4075) based on the strong-CF scheme for Ni^{2+} ions in $LiNbO_3$ crystals. The correctness of our CFA/MSH package is verified by comparing our results with the predictions of Ma *et al* (Ma D P, Ma N, Ma X D and Zhang H M 1998 *J. Phys. Chem. Solids* **59** 1211, Ma D P, Ma X D, Chen J R and Liu Y Y 1997 *Phys. Rev. B* **56** 1780) and Macfarlane (Macfarlane R M 1964 *J. Chem. Phys.* **40** 373) for $\alpha-Al_2O_3 : V^{3+}(3d^2)$ and $MgO : Ni^{2+}(3d^8)$. It appears that the two independent approaches show perfect agreement with our approach, unlike those of Zhou *et al* and Li, which turn out to be unreliable. Our results reveal that the contributions to the ZFS parameter from the higher excited states cannot be neglected; also, the ZFS parameter is very sensitive to slight changes of the crystal structure. Hence our CFA/MSH package, which takes into account the contributions to the ZFS parameter from the higher excited states, can provide reliable results and proves to be a useful tool for the studies of the effect of the lattice distortions, defects and structural disorder on the spectroscopic properties of $3d^2$ and $3d^8$ ions at trigonal symmetry sites in crystals.

1. Introduction

Since its inception by Pryce [1] the microscopic spin Hamiltonian (MSH) theory has been extensively used in the area of the electron paramagnetic resonance (EPR) of transition ions (for a review, see e.g. [2–5]). The MSH theory enables correlation of the optical spectroscopy and structural data with the spin-Hamiltonian (SH) parameters extracted from the EPR spectra. Hence, the MSH studies of the transition-metal ions in crystals can provide a great deal of microscopic insight concerning the crystal structure, structural disorder, phase transitions and pressure behaviour as well as the observed magnetic and spectroscopic properties. There are two major approaches to the microscopic derivation of the SH parameters, namely the complete diagonalization method (CDM) and the perturbation theory method (PTM). The PTM (historically first) takes into account the contributions to the SH parameters from a selected subset of the $3d^N$ excited states within the ligand-field framework (for a review, see e.g. [2–4]). Advances in the computational techniques in the last several decades have enabled development of the CDM by various authors. The CDM takes into account the contributions from all $3d^N$ excited states and hence can provide more accurate determination of the SH parameters. The CDM has, however, some limitations for symmetries lower than axial since the number of available ZFS transitions obtained from CDM may be insufficient to determine all non-zero ZFS parameters predicted by group theory for these symmetry cases [3,4].

Both PTM and CDM have been extensively used to investigate the SH parameters of $3d^2$ and $3d^8$ ions with the ground orbital singlet state $^3A_2(^3F)$ at axial symmetry sites. To explain the axial zero-field splitting (ZFS) parameter D and the anisotropic g -factors, g_{\parallel} and g_{\perp} , for Ni^{2+} and Cu^{3+} in some crystals, Blumberg *et al* [6] and Kamimura [7] derived perturbation formulae, taking into account only the contributions to the SH parameters from the nearest excited $^3T_2(^3F)$ states. However, the investigations [8] revealed that the PTMs [6,7] were inadequate, since the wrong signs of D and $\Delta g = (g_{\parallel} - g_{\perp})$ were obtained [8]. In order

to improve the PTMs [6, 7], ‘quasi-fourth-order’ perturbation formulae have been derived by Petrosyan and Mirzakhanyan (PM) [8]. Some shortcomings of the PTM of PM [8] were discussed by Zhou *et al* [9], who developed a CDM for calculation of the SH parameters for 3d⁸ ions in C_{3v} symmetry using the strong-CF scheme. Recently, the CDM results [9] were criticized as incorrect by Li [10], who independently developed a similar CDM. An alternative CDM has also been developed by Ma *et al* [11, 12]; however, they have not commented on the CDM results of Zhou *et al* [9] and Li [10].

The contradictory results [8–10] and the controversial claims [10] require a thorough analysis. The present investigations have been aimed at solving the controversy and providing a comparative analysis of the validity of the existing MSH approaches [6–13]. To this end, as an extension of our previous crystal-field analysis (CFA) package for 3d^N ions [14–16], we have recently incorporated the MSH approach to form a task-specific CFA/MSH package to calculate the SH parameters for 3d⁸(3d²) ions with an orbital singlet ground state at trigonal (C_{3v}, D₃, D_{3d}) symmetry sites. Our approach adopts the intermediate CF scheme and takes into account the contributions to the SH parameters from 45 states of 3d⁸ (or 3d²) ions. In section 2 we provide briefly the basic theoretical background for the CFA and CFA/MSH computer packages. The results of extensive numerical calculations using our CFA/MSH package are presented in section 3. *First*, the selection of the input parameters for a wide range of values is outlined and the dependence of the SH parameters on the CF ones is studied. This enables quantitative analysis of the predictions of the PTM [8] for Ni²⁺ ions in LiNbO₃ crystals. *Second*, the numerical calculations for 3d² and 3d⁸ ions at C_{3v} symmetry sites in several crystals are worked out. The results provide a basis for comparative analysis of the validity of the existing MSH approaches based on the CDM [9–13] and hence solving the above controversy [9, 10]. It turns out that the results of Zhou *et al* [9] and Li [10] appear to be incorrect, most probably due to errors in their matrix elements. A summary and conclusions are provided in section 4.

2. Crystal-field and microscopic spin Hamiltonian theory

2.1. Crystal-field analysis (CFA) package

In the crystal-field (CF) framework, the Hamiltonian for the transition-metal 3d^N ions in a crystal can be written as (see e.g. [17, 18])

$$H = H_{ee}(B, C) + H_{SO}(\xi) + H_{Trees}(\alpha) + H_{CF}(B_{kq}), \quad (1)$$

where H_{ee} , H_{SO} , H_{Trees} and H_{CF} represent, respectively, the Coulomb interactions, the spin-orbit (SO) coupling, the Trees correction describing the two-body orbit-orbit polarization interaction [19] and the CF interaction. In the CFA package [14–16] we employ H_{CF} in the Wybourne notation [20]:

$$H_{CF} = \sum_{k,q} B_{kq} C_q^{(k)} \quad (2)$$

where B_{kq} are the CF parameters with $k = 2$ and 4 for the transition-metal ions. For trigonal (C_{3v}, D₃, D_{3d}) symmetry $q = 0, \pm 3$ and all CF parameters are real. For convenience and unification of CF datasets, we also use the relationships between B_{kq} in equation (2) and the conventional CF parameters as given in table 4 of [14] (see also [21, 22] and references therein):

$$\begin{aligned} B_{20} &= v - 2\sqrt{2}v' \\ B_{40} &= -14Dq + 2w/3 \\ B_{43} &= -\sqrt{7/10}(20Dq + w/3) \end{aligned} \quad (3)$$

where $w = 2v + 3\sqrt{2}v'$, Dq is the cubic parameter and the parameters v and v' measure the net trigonal CF components and vanish identically in cubic symmetry [23, 24]. Note that equation (3) is only applicable for the F-term ions (e.g. d^2 and d^8) [14] in trigonal symmetry.

Since for most $3d^N$ ions in crystals the CF is of intermediate strength, the basis functions in the LS -coupling scheme have been adopted [14–16]:

$$|\varphi\rangle = |d^N \alpha L S M_L M_S\rangle \quad (4)$$

where α is an extra quantum number. Details concerning the choice of the basis functions and the techniques for calculation of the matrix elements can be found in [14–16]. For $3d^2$ ions having threefold site symmetry such as the trigonal (C_{3v} , D_3 , D_{3d}) symmetry, the matrices of Hamiltonians in equation (1) are of the dimension 45×45 and can be partitioned into three smaller matrices, each of the dimension 15×15 . The equivalence between the $(10 - N)$ -electron systems and the N -hole systems (see e.g. [25]), resulting in the change of the sign of the matrix elements of the CF and SO coupling interaction terms, is built internally into the CFA package [14–16], and hence the complete Hamiltonian matrix can be obtained for both the $3d^8$ and $3d^2$ ions automatically. Full diagonalization of each energy matrix for trigonal symmetry leads to mixing of all 15 states by the SO coupling. Hence, the eigenvectors $|\psi_j\rangle$ are obtained as a linear combination of the LS basis functions defined in equation (4) above:

$$|\psi_j\rangle = \sum_{i=1}^{15} a_{ji} |\varphi_i\rangle, \quad (5)$$

where a_{ji} are the respective mixing coefficients within the full $3d^2(3d^8)$ configuration. It is worthwhile to point out that the eigenvectors of the type in equation (5) are particularly suitable for calculation of the Zeeman g -factors as well as the ZFS for the ground orbital singlet arising from the F-term (e.g. $3d^2$ or $3d^8$ and $3d^3$ or $3d^7$) as well as the S-term (e.g. $3d^5$) in crystals [14, 22].

The CFA computer package for $3d^N$ ions [14–16] has recently been converted by one of us (YYY) from the QuickBasic 4.5 version under DOS into the Visual Basic 6.0 version under the Microsoft Windows environment. Then, a separate CFA/MSH package was developed for microscopic calculations of the ZFS parameter D and the g -factors (g_{\parallel} , g_{\perp}) for $3d^8$ and $3d^2$ ions at trigonal (C_{3v} , D_3 , D_{3d}) symmetry sites as a function of the CF parameters. This package employs the CDM described in section 2.2. At a later stage the present version of the CFA/MSH package will be extended to include the electronic spin–spin [2, 5] and spin–other-orbit [14] interactions as well as the Zeeman terms for any $3d^N$ ion at arbitrary symmetry.

2.2. Determination of the SH parameters using the CFA/MSH package

The free-ion 3F ground term of $3d^8$ ions (e.g. Ni^{2+}) splits in octahedral symmetry into 3A_2 , 3T_2 and 3T_1 states, whereas the excited terms, one 3P and the three 1X (1S , 1D , 1G), split into various CF levels. Due to the combined action of the axial CF and SO coupling, all excited terms are mixed up, to a varying degree, with the ground 3F term, making the ground 3A_2 state no longer a pure spin triplet state. Moreover, the 3A_2 state is then further split into the *effective* [3–5] spin singlet state $|A_1(^3F \downarrow ^3A_2 \downarrow ^3A_2)\rangle$ and doublet state $|E_{\pm 1}(^3F \downarrow ^3A_2 \downarrow ^3A_2)\rangle$ (see figure 1), which can be labelled by the *effective* spin [3–5] quantum number $\tilde{M}_S = 0$ and ± 1 , respectively (see below). Here, we use the notation $|\Gamma_{C_{3v}}^*(2S+1L \downarrow 2S+1\Gamma_{O_h} \downarrow 2S+1\Gamma_{C_{3v}})\rangle$ to label final states, since it shows explicitly the parentage of the states arising from the combined action of H_{SO} and $H_{CF}(C_{3v})$. Hence, the magnetic properties of the ground state of $3d^8$ ($3d^2$) ions depend upon the mixing of the higher CF levels into the ground state by the SO coupling and lower symmetry CF terms. The energy difference Δ between the states $|E_{\pm 1}(^3F \downarrow ^3A_2 \downarrow ^3A_2)\rangle$

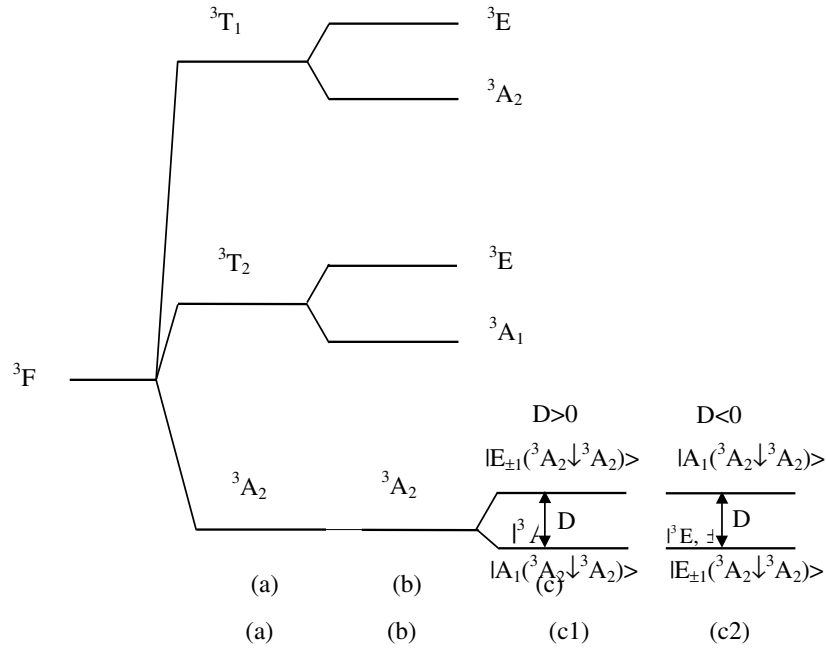


Figure 1. Schematic splitting of the ground term for 3d⁸ ions: (a) V_c (cubic CF), (b) $V_c + V_{trig}$ (trigonal CF), (c) $V_c + V_{trig} + H_{so}$ (SO coupling); two options for the sign of the ZFS parameter D are indicated.

and $|A_1(^3F \downarrow ^3A_2 \downarrow ^3A_2)\rangle$ can be equivalently described by the *effective* SH (for a review, see [3, 4]). This Δ is actually equal to the ZFS parameter D , which can be measured by EPR spectroscopy. The ground states $|E_{+1}(^3F \downarrow ^3A_2 \downarrow ^3A_2)\rangle$, $|E_{-1}(^3F \downarrow ^3A_2 \downarrow ^3A_2)\rangle$ and $|A_1(^3F \downarrow ^3A_2 \downarrow ^3A_2)\rangle$, which are denoted by $|\Psi_{+1}\rangle$, $|\Psi_{-1}\rangle$, and $|\Psi_0\rangle$, respectively, are obtained by complete diagonalization of the three 15×15 matrices using the CFA package in the form of linear combinations in equation (5).

In an external magnetic field \mathbf{B} , the energy levels will be further split by the electronic Zeeman interaction [2]:

$$H_{Ze} = \mu_B(k\mathbf{L} + g_e\mathbf{S}) \cdot \mathbf{B} \quad (6)$$

where k is the orbital reduction factor describing the covalence and overlap effects on the orbital angular momentum \mathbf{L} , \mathbf{S} is the *true* electronic spin angular momentum, μ_B is the Bohr magneton and $g_e = 2.0023$. For 3d⁸(3d²) ions in trigonal symmetry, the appropriate *effective* SH [3, 4], including the ZFS and Zeeman terms, is [2]

$$H_S = H_{ZFS} + H_{Ze} = D[S_z^2 - \frac{1}{3}S(S+1)] + \mu_B g_{\parallel} B_z S_z + \mu_B g_{\perp} (B_x S_x + B_y S_y) \quad (7)$$

where D is the ZFS parameter and g_{\parallel} and g_{\perp} are the Zeeman g -factors. The spin operators in equation (7) are the *effective* spin \tilde{S} operators [3–5]; however, for simplicity the ‘tilde’ is omitted, unlike in \tilde{M}_S used above.

Using the MSH theory [23, 24], we obtain the Zeeman g -factors and ZFS parameter D as follows:

$$\begin{aligned} g_{\parallel} &= k\langle\psi_{+1}|L_0^{(1)}|\psi_{+1}\rangle + g_e\langle\psi_{+1}|S_0^{(1)}|\psi_{+1}\rangle \\ g_{\perp} &= k(\langle\psi_{+1}|L_{-1}^{(1)}|\psi_0\rangle - \langle\psi_{+1}|L_{+1}^{(1)}|\psi_0\rangle) + g_e(\langle\psi_{+1}|S_{-1}^{(1)}|\psi_0\rangle - \langle\psi_{+1}|S_{+1}^{(1)}|\psi_0\rangle) \end{aligned} \quad (8)$$

$$D = \varepsilon(|E(^3F \downarrow ^3A_2 \downarrow ^3A_2)\rangle) - \varepsilon(|A_1(^3F \downarrow ^3A_2 \downarrow ^3A_2)\rangle) \quad \text{for } 3d^8 \text{ ion} \quad (9a)$$

$$D = \varepsilon(|E(^3F \downarrow ^3T_1 \downarrow ^3A_2)\rangle) - \varepsilon(|A_1(^3F \downarrow ^3T_1 \downarrow ^3A_2)\rangle) \quad \text{for } 3d^2 \text{ ion} \quad (9b)$$

where the rank-one operators are defined according to the Racah convention for the irreducible tensor operators [26, 27],

$$\begin{aligned} L_{\pm 1}^{(1)} &= \mp \frac{1}{\sqrt{2}}(L_x \pm iL_y) = \mp \frac{1}{\sqrt{2}}L_{\pm}, & L_0^{(1)} &= L_z \\ S_{\pm 1}^{(1)} &= \mp \frac{1}{\sqrt{2}}(S_x \pm iS_y) = \mp \frac{1}{\sqrt{2}}S_{\pm}, & S_0^{(1)} &= S_z. \end{aligned} \quad (10)$$

The major steps of our present CDM calculations for the g -factors and ZFS parameters D in equations (8) and (9) are concisely outlined as follows:

- (i) The mixing coefficients for the wavefunctions of the three relevant states were obtained from the CFA package [14–16] as some linear combinations of the LS wavefunctions $|\varphi_i\rangle$ defined in equation (4), i.e.

$$|\psi_m\rangle = \sum_{i=1}^{15} a_{mi} |\varphi_i\rangle, \quad (11)$$

where $m = 0$ and ± 1 (i.e. the *effective* \tilde{M}_S) correspond to the states $|A_1(^3F \downarrow ^3A_2 \downarrow ^3A_2)\rangle$ for $3d^8$ ion ($|A_1(^3F \downarrow ^3T_1 \downarrow ^3A_2)\rangle$ for $3d^2$) and $|E_{\pm 1}(^3F \downarrow ^3A_2 \downarrow ^3A_2)\rangle$ for $3d^8$ ion ($|E_{\pm 1}(^3F \downarrow ^3T_1 \downarrow ^3A_2)\rangle$ for $3d^2$ ion), respectively, and every index i in equation (11) refers a different set of the $\alpha LSM_L M_S$ quantum numbers.

- (ii) The matrix elements of the irreducible tensor operators defined in equation (10) were calculated from the following two equations:

$$\langle \varphi_i | L_q^{(1)} | \varphi_j \rangle = (-1)^{L-M_L} (L(L+1)(2L+1))^{\frac{1}{2}} \begin{pmatrix} L & 1 & L' \\ -M_L & q & M'_L \end{pmatrix} \delta_{\alpha\alpha'} \delta_{LL'} \delta_{SS'} \delta_{M_S M'_S} \quad (12a)$$

$$\langle \varphi_i | S_q^{(1)} | \varphi_j \rangle = (-1)^{S-M_S} (S(S+1)(2S+1))^{\frac{1}{2}} \begin{pmatrix} S & 1 & S' \\ -M_S & q & M'_S \end{pmatrix} \delta_{\alpha\alpha'} \delta_{LL'} \delta_{SS'} \delta_{M_L M'_L}, \quad (12b)$$

where (...) are the $3j$ symbols and δ is the Kronecker delta. In deriving the above two equations, we have employed the Wigner–Eckart theorem together with the closed form for the reduced matrix elements of the orbital angular momentum tensor operator L , i.e.

$$\langle \alpha LS \| L \| \alpha' L' S' \rangle = \delta_{\alpha\alpha'} \delta_{LL'} \delta_{SS'} (L(L+1)(2L+1))^{\frac{1}{2}}, \quad (13)$$

and a similar expression for the spin angular momentum operator S .

- (iii) Our present CFA/MSH package was used to compute the matrix elements for g_{\parallel} and g_{\perp} in equation (8) using equations (11) and (12a, b), i.e.

$$\langle \psi_{+1} | S_0^{(1)} | \psi_{+1} \rangle = \sum_{i,j}^{15} a_{+1,i}^* a_{+1,j} \langle \varphi_i | S_0^{(1)} | \varphi_j \rangle \quad (14a)$$

$$\langle \psi_{+1} | S_{\pm 1}^{(1)} | \psi_0 \rangle = \sum_{i,j}^{15} a_{+1,i}^* a_{0,j} \langle \varphi_i | S_{\pm 1}^{(1)} | \varphi_j \rangle \quad (14b)$$

$$\langle \psi_{+1} | L_0^{(1)} | \psi_{+1} \rangle = \sum_{i,j}^{15} a_{+1,i}^* a_{+1,j} \langle \varphi_i | L_0^{(1)} | \varphi_j \rangle \quad (14c)$$

$$\langle \psi_{+1} | L_{\pm 1}^{(1)} | \psi_0 \rangle = \sum_{i,j}^{15} a_{+1,i}^* a_{0,j} \langle \varphi_i | L_{\pm 1}^{(1)} | \varphi_j \rangle. \quad (14d)$$

- (iv) From the eigen-energies of the states $|A_1(^3F \downarrow ^3A_2 \downarrow ^3A_2)\rangle$ for 3d⁸ ion ($|A_1(^3F \downarrow ^3T_1 \downarrow ^3A_2)\rangle$ for 3d²) and $|E_{\pm 1}(^3F \downarrow ^3A_2 \downarrow ^3A_2)\rangle$ for 3d⁸ ion ($|E_{\pm 1}(^3F \downarrow ^3T_1 \downarrow ^3A_2)\rangle$ for 3d² ion) as generated from the CFA package, the ZFS parameter D was easily obtained according to equation (9).

Since the CFA/MSH package includes the contributions from all 45 states for 3d⁸(3d²) ions, it is used in section 2.3 to check the convergence of the PTM formulae for the SH parameters [6, 8], which include only the contributions from some excited states.

2.3. Perturbation theory of MSH

The authors of [8] have derived for 3d⁸ ions in trigonal symmetry the approximate perturbation formulae for the SH parameters D , g_{\parallel} and g_{\perp} in terms of the SO coupling parameter ξ , the orbital reduction factor k and the trigonal CF parameters v and v' as well as the energy denominators W_i , $i = 1-5$. Hence, only the contributions from these five excited states have been taken into account in the PTM [8], as pointed out in [9]. The relations for W_i , in terms of the cubic CF parameter $10Dq$ and Racah parameters B and C , and the perturbation formulae of [8], have been built up by us into a Visual Basic program for numerical calculations to enable comparison of the PTM and CDM results in section 3. Since all relevant papers [8–13] use the conventional CF parameters Dq , v and v' , in the following studies we shall uniformly use these parameters for presentation of the results of the CDM and PTM calculations.

3. Numerical results

3.1. CFA/MSH predictions of the dependence of SH parameters on the CF ones

Using the CFA/MSH package, the SH parameters D , g_{\parallel} and g_{\perp} can be systematically studied as functions of the CF parameters. The dependence of the SH parameters on the CF parameters v , v' and Dq predicted by our CFA/MSH package for 3d⁸ ions in trigonal symmetry is plotted in figures 2–5 for the SH parameters D , g_{\parallel} , g_{\perp} and Δg ($\Delta g = g_{\parallel} - g_{\perp}$), respectively. A table providing the numerical data corresponding to figures 2(c)–5(c), i.e. the SH parameters (D , g_{\parallel} , Δg) for selected values of Dq pertinent for Cu³⁺ ion at trigonal symmetry, which shows explicitly the quantitative relationship between the CDM and PTM results (see section 3.2), is available from the authors upon request. The model calculations were carried out using the input parameters in the range pertinent for Cu³⁺ and, to a certain extent, for Ni²⁺ ions. The Racah parameters were fixed as $B = 1030 \text{ cm}^{-1}$ and $C = 4850 \text{ cm}^{-1}$ [8]. Keeping in mind the data available in the literature, $v = -2400 \text{ cm}^{-1}$ for Ni²⁺: LiNbO₃ [9], $Dq = 2100 \text{ cm}^{-1}$ for Cu³⁺: Al₂O₃ [8] and $Dq = 775 \text{ cm}^{-1}$ for Ni²⁺: α -LiIO₃ [8], in order to cover a wide range of the CF parameter values we have chosen between -3000 and 3000 cm^{-1} for v and v' and 400 – 2400 cm^{-1} for Dq . The SO coupling constant ξ has been taken as 600 cm^{-1} , pertinent for the Cu³⁺ ion [8]. Another choice for the possible parameter values would not affect the conclusions drawn below.

It can be seen from figures 2 and 5 that the values of D (see figures 2(a) and (b)) and Δg (see figures 5(a) and (b)) strongly depend on the trigonal CF parameter v' , whereas they are not very sensitive to v . Similar findings for the 3d³ ions in trigonal symmetry have been pointed out in [23, 24, 28]; for example, Macfarlane [23] obtained the relation $D \approx -4.5 \times 10^{-10} \xi^2 v + 7.2 \times 10^{-9} \xi^2 v'$ for the Cr³⁺ ions at octahedral sites. Figures 2(c)–5(c) and table 1 also indicate that D , g_{\parallel} , g_{\perp} and Δg are very sensitive to the changes of Dq in the range $400 \text{ cm}^{-1} \leq Dq < 1000 \text{ cm}^{-1}$, whereas they are not so sensitive in the range

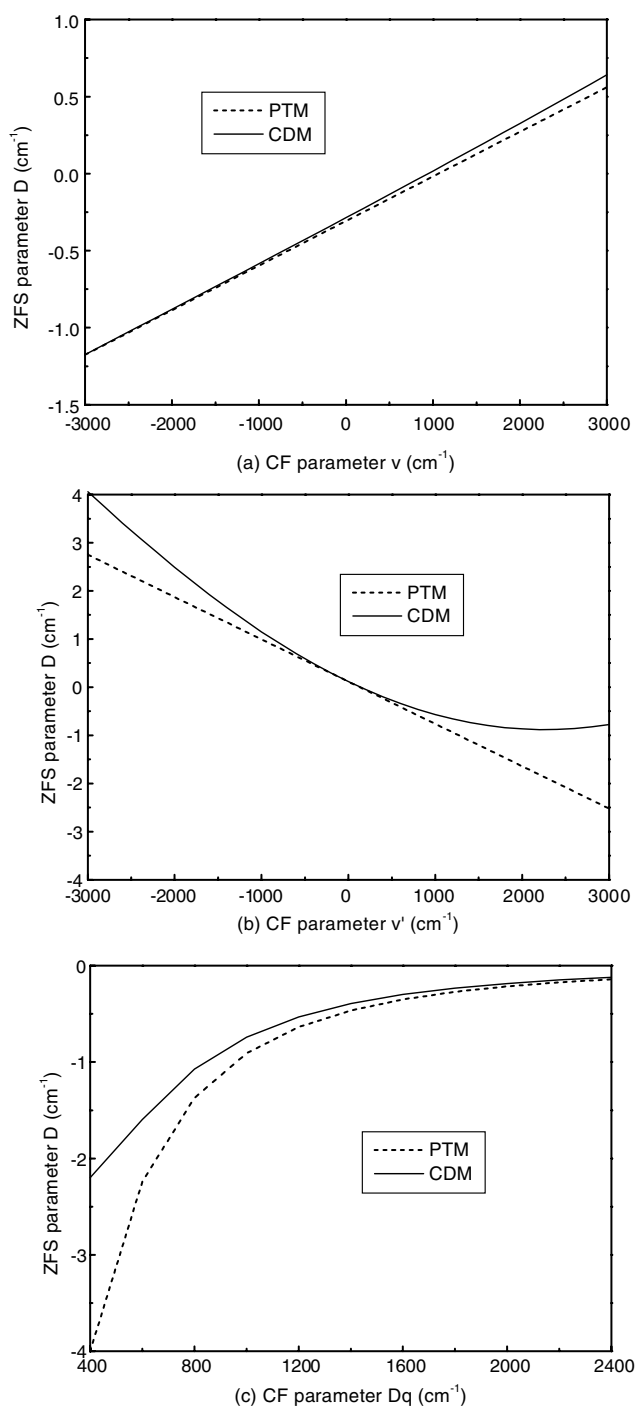


Figure 2. ZFS parameter D for the ground state of the $3d^8$ ion in C_{3v} symmetry versus (a) v ($v' = 350$, $B = 1030$, $C = 4850$, $\zeta = 600$, $Dq = 2100$), (b) v' ($v = 400$, $B = 1030$, $C = 4850$, $\zeta = 600$, $Dq = 2100$) and (c) Dq ($v' = 350$, $v = 400$, $B = 1030$, $C = 4850$, $\xi = 600$). Solid curves, present CDM results; dashed curves, calculated by us using the PTM expressions of [8]; all values in (cm^{-1}).

$1000 \leq Dq \leq 2400 \text{ cm}^{-1}$. The Dq of the Cu^{3+} ion (e.g. $Dq = 2100 \text{ cm}^{-1}$ for $\text{Cu}^{3+} : \text{Al}_2\text{O}_3$) is generally larger than that of the Ni^{2+} ion (e.g. $Dq = 775 \text{ cm}^{-1}$ for $\text{Ni}^{2+} : \alpha\text{-LiIO}_3$). Thus the SH parameters are sensitive to Dq for Ni^{2+} ions, whereas they are not for Cu^{3+} ions.

3.2. Comparisons of the CFA/MSH and PTM results

In order to check the accuracy of the PTM [8] predictions of D , g_{\parallel} and g_{\perp} , both the present CFA/MSH results and those obtained by us using the PTM formulae [8] are also shown in figures 2–5. From figures 2–5, we conclude as follows.

- (i) Our numerical calculations show that D and Δg reverse sign in a correlated way, i.e. for $D < 0$, $\Delta g > 0$, whereas for $D > 0$, $\Delta g < 0$. A similar conclusion is obtained using the approximate relation $D \approx -(1/4)\xi\Delta g$ [8]. Since the present CFA/MSH calculations are based on the CDM, they provide a justification for this approximation.
- (ii) Comparison of the results obtained by us using the PTM [8] and our CDM (see figures 3–5) reveals that the g -factors predicted by the PTM are in agreement with those obtained from our CDM, especially for the cases of small v and v' and large Dq . However, the PTM predictions of the ZFS parameter D (see figure 2) show appreciable differences as compared with the CDM ones. The numerical calculations show that the percentage difference varies from about 16% for $Dq = 2400 \text{ cm}^{-1}$ to about 86% for $Dq = 400 \text{ cm}^{-1}$. Due to these shortcomings, the PTM [8] can be only used for *approximate* estimations of the SH parameters in the range $Dq > 800$, $-1000 < v' < 1000$ and $-3000 < v < 2000$ (in cm^{-1}).
- (iii) The perturbation formulae [8] for D , g_{\parallel} and g_{\perp} include only the contributions from the five lower excited states (${}^3\text{T}_2$, ${}^3\text{T}_1$, ${}^1\text{T}_2$, ${}^3\text{T}_1$ and ${}^1\text{T}_2$). Thus the observed good agreement between the PTM and CDM results indicate that the contributions to g_{\parallel} and g_{\perp} originate mainly from the lower excited states. However, in the case of D the observed disagreement indicates that the higher excited states play a very important role, especially for Ni^{2+} ions experiencing a smaller Dq . Thus the contributions to D from the higher excited states cannot be neglected.

For concrete applications, in table 1 we present the values of D , g_{\parallel} and Δg , calculated using our CMD and the PTM [8] for Cu^{3+} and Ni^{2+} in Al_2O_3 , $\alpha\text{-LiIO}_3$ and LiNbO_3 crystals, which exhibit a trigonally distorted octahedral CF. This enables meaningful comparison between the results of our CDM and those of the PTM [8]. Note that in tables 1–3 we retain the number of significant digits for the values calculated by us to match the number used for the corresponding experimental and/or theoretical values of others, which are quoted as in the original for comparison. In tables 2 and 3 the states are labelled by irreducible representations of the respective point symmetry group (without H_{SO}) and the double group—indicated by an asterisk (taking into account H_{SO}). For simplicity the part (${}^{2S+1}L$) is omitted in the notation used in tables 2 and 3. Table 1 reveals that for both Cu^{3+} and Ni^{2+} ions in these crystals, the g -factors obtained by us using the perturbation formulae [8] are close to those evaluated by our CDM. The respective results for the ZFS parameter D show discrepancies between the results of the two methods, especially for the Ni^{2+} ion. These discrepancies may be due to the weaker CF strength: $Dq(\text{Ni}^{2+}) \approx (1/2)Dq(\text{Cu}^{3+})$. Since the accuracy of the SH parameters obtained by the PTM decreases with decreasing Dq , the validity of the PTM [8] in the range of Dq pertinent for the Ni^{2+} ion may be questionable (see table 1).

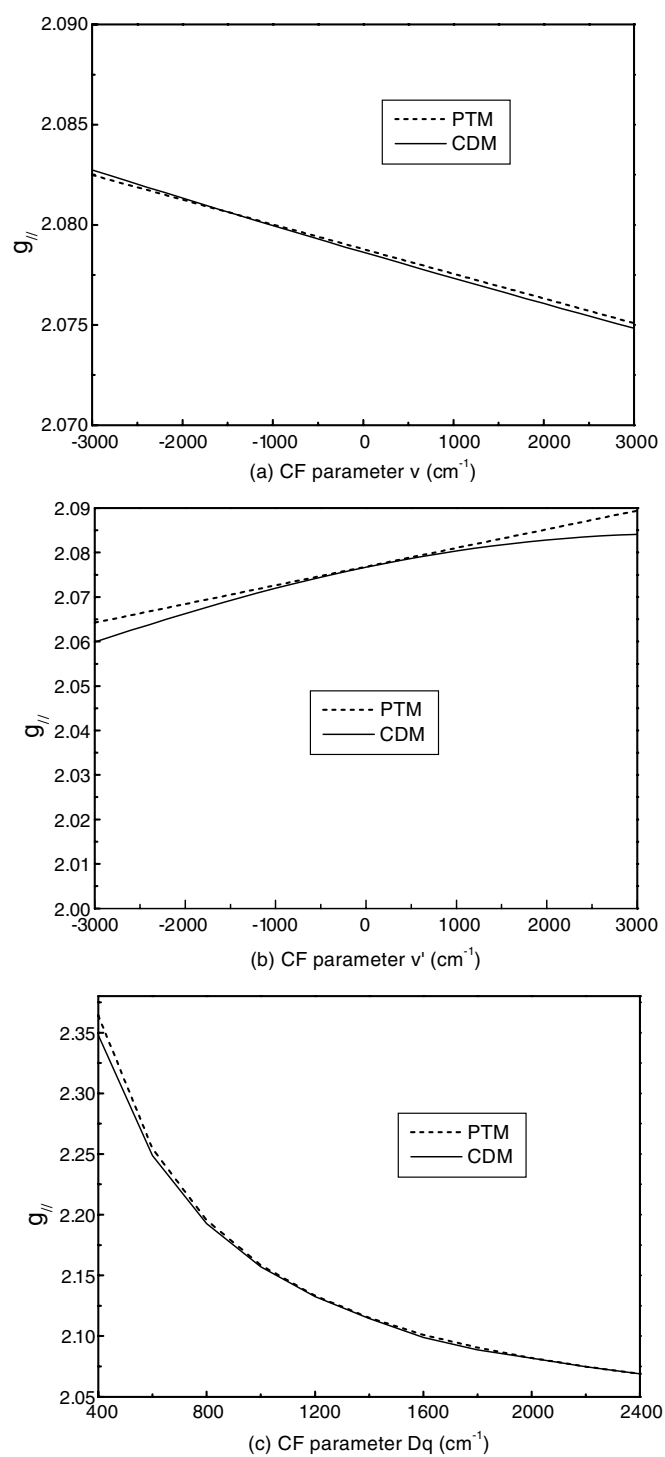


Figure 3. Zeeman parameter $g_{||}$ for the ground state of the $3d^8$ ion in C_{3v} symmetry versus (a) v , (b) v' and (c) Dq . The orbital reduction factor $k = 0.68$; other parameters are as shown in figure 2. Solid and dashed curves have the same meaning as in figure 2.

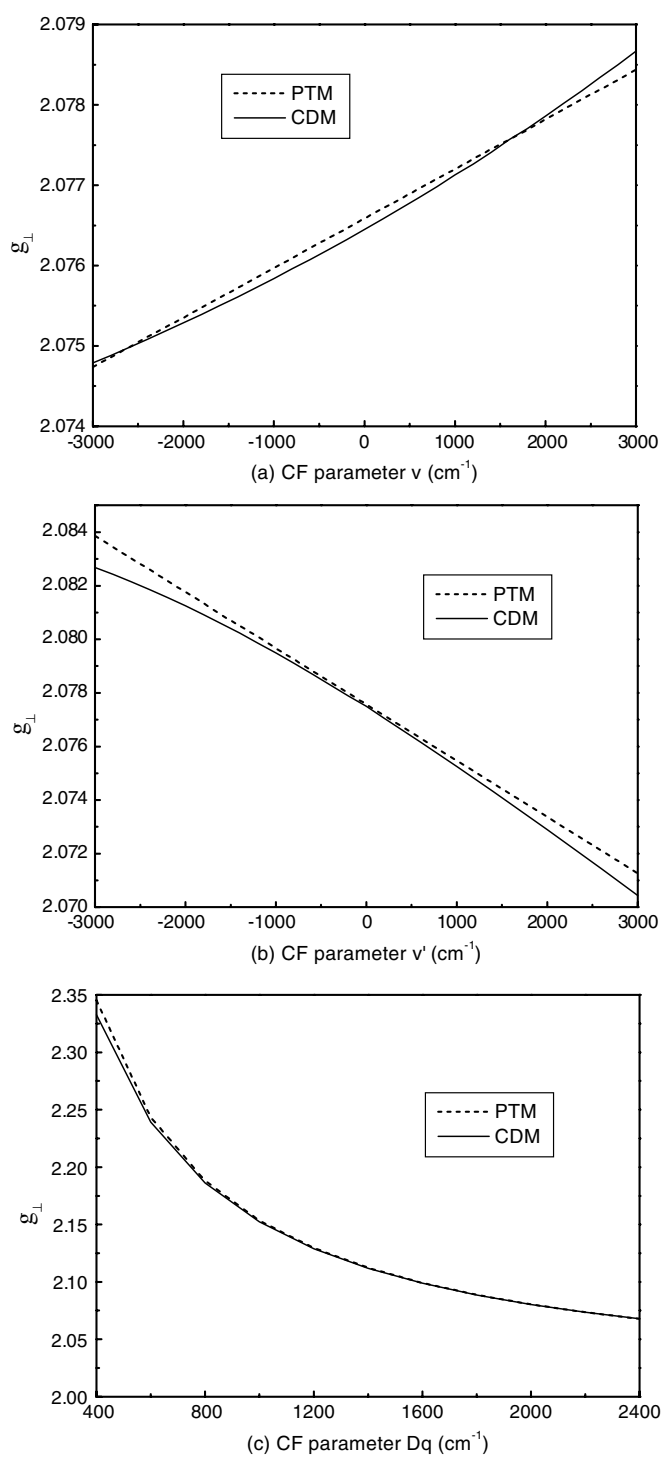


Figure 4. Zeeman parameter g_{\perp} for the ground state of the $3d^8$ ion in C_{3v} symmetry versus (a) v , (b) v' and (c) Dq . The orbital reduction factor $k = 0.68$; other parameters are as shown in figure 2. Solid and dashed curves have the same meaning as in figure 2.

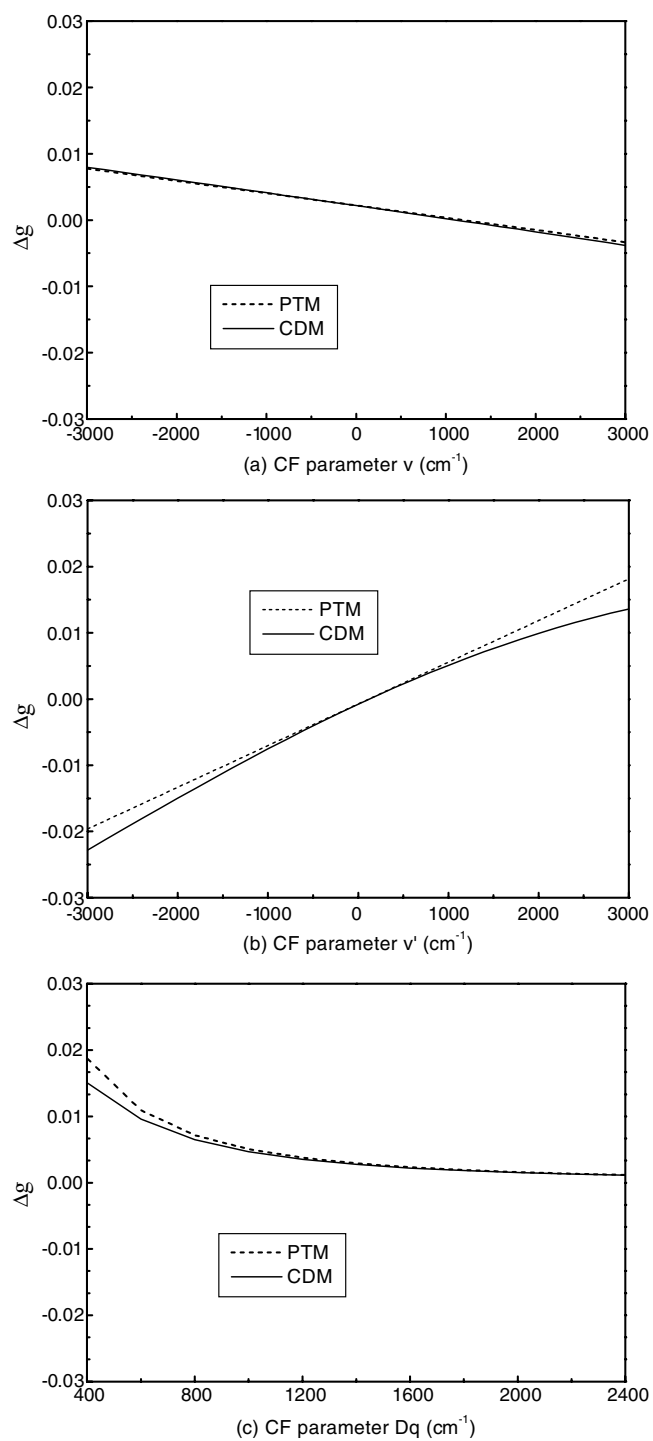


Figure 5. Zeeman parameter $\Delta g = g_{\parallel} - g_{\perp}$ for the ground state of the $3d^8$ ion in C_{3v} symmetry versus (a) v , (b) v' and (c) Dq . The orbital reduction factor $k = 0.68$; other parameters are as shown in figure 2. Solid and dashed curves have the same meaning as in figure 2.

Table 1. Calculated and experimental values of the SH parameters for 3d⁸ ions in several crystals with C_{3v} site symmetry. All values in cm⁻¹ except for k , g_i and Δg .

SH parameter	Al ₂ O ₃ : Cu ³⁺ ^c	Al ₂ O ₃ : Ni ²⁺ ^d	α -LiIO ₃ : Ni ²⁺ ^e	LiNbO ₃ : Ni ²⁺ ^f
D^a	-0.195	-1.14	-2.85	-5.24
D^b	-0.165	-0.74	-2.65	-4.83
$D_{exp.}$ [8]	-0.188	-1.38	-3.21	-5.31 (-5.07 \pm 0.01 ^g)
g_{\parallel}^a	2.0789	2.1958	2.281	2.239
g_{\parallel}^b	2.0781	2.1921	2.2768	2.2374
$g_{\parallel exp.}$ [8]	2.0788	2.1957	2.280	2.24 (2.24 \pm 0.03 ^g)
Δg^a	0.0015	0.0094	0.021	0.038
Δg^b	0.0014	0.0078	0.0201	0.0384
$\Delta g_{exp.}$ [8]	0.0016	0.0098	0.023	0.04

^a Calculated by us using the PTM expressions of [8].

^b Present CDM results.

^c $B = 1030$, $C = 4850$, $Dq = 2100$, $\xi = 600$, $v = 400$, $v' = 350$ and $k = 0.68$ [8].

^d $B = 800$, $C = 3400$, $Dq = 1000$, $\xi = 565$, $v = 600$, $v' = 500$ and $k = 0.87$ [8].

^e $B = 850$, $C = 3600$, $Dq = 775$, $\xi = 595$, $v = -550$, $v' = 200$ and $k = 0.92$ [8].

^f $B = 816$, $C = 3224$, $Dq = 792$, $\xi = 540$, $v = -950$, $v' = 600$ and $k = 0.83$ [8].

^g Reference [40] recalculated from 152.1 ± 0.3 GHz using $1 \text{ GHz} = 0.033 \text{ 356 cm}^{-1}$.

3.3. The validity of other CDM results

Zhou *et al* [9] calculated the energy levels, the ZFS parameter D and g -factors for Ni²⁺ ions in LiNbO₃ crystals employing the CDM based on the strong-CF scheme. Recently, the results [9] were criticized as incorrect by Li [10], who also used the strong-CF scheme. In order to solve this controversy, it is necessary to check the validity of the CDM used by Zhou *et al* [9] and Li [10]. Substituting the two sets ((A) [9, 10] and (B) [8]) of spectroscopic parameters as input into our CFA/MSH package, we obtain the SH parameters and energy levels listed in table 2. It can be seen from table 2 that the results of [9, 10] disagree with each other and with those obtained using our CFA/MSH package. Using set (A) Zhou *et al* [9] obtained $D = 5.073 \text{ 19 cm}^{-1}$ and $\Delta g = -0.0057$, neither of which agrees well with the experimental values in magnitudes and signs (see table 2). Substituting set (B) into our CFA/MSH package, we obtain $D = -4.829 \text{ cm}^{-1}$, $g_{\parallel} = 2.2374$ and $\Delta g = 0.0383$, which roughly agree with the experimental values (see table 2). Hence, contrary to the criticism by Zhou *et al* [9] of set (B) as unreasonable, the spectroscopic parameters determined by PM [8] (i.e. set (B)) are rather acceptable. Note that the theory presentation and notation used by Li [10] is rather awkward and there are some inconsistencies (see our table 2) in the energy level values listed in her table 1 (last column) and table 2 (first column), which should be identical.

In view of the above discrepancies and in order to ensure the validity of our CFA/MSH package, we have thoroughly rechecked our CFA and CFA/MSH packages. No errors have been found. Confirmation of the validity of our computer package arises from comparison with the recent results of Ma *et al* [11, 12], who have independently developed the CDM for 3d²(3d⁸) ions in trigonal symmetry based on the *strong*-CF scheme. Their CDM has been used to study the pressure-induced shifts of the energy levels of MgO : Ni²⁺(3d⁸) [12] and α -Al₂O₃ : V³⁺(3d²) [11]. Additionally, we have checked the results against those of Macfarlane [13], who used the CDM based on the *weak*-CF scheme for α -Al₂O₃ : V³⁺(3d²). Substituting the three sets of parameters, C [11], D [13] and E [12], into our CFA/MSH package, we obtain the SH parameters and energy levels listed in table 3. It is evident that both the energy levels and the SH parameters calculated by us agree very well with those of Ma *et al* [11, 12] and Macfarlane [13]. This extensive agreement proves that the independently

Table 2. Comparison between the energy levels and SH parameters calculated using the present CDM/MSH package and other CDMs for the Ni^{2+} ion in LiNbO_3 crystals. All values in cm^{-1} except for k , g_i and Δg . Set (A): $B = 790$, $Dq = 830$, $C = 3270$, $\xi = 530.5$, $v = -2400$, $v' = 565.69$, $k = 1$ [9]. Set (B): $B = 816$, $Dq = 792$, $C = 3224$, $\xi = 540$, $v = -950$, $v' = 600$, $k = 0.83$ [8].

Assignment C_{3v}^* ($O_h \downarrow C_{3v}$)	Expt [43]	Set (A)			Set (B)		
		This work ^a	Zhou <i>et al</i> ^b [9]	Li ^c [10]	This work ^d	Zhou <i>et al</i> ^e [9]	Li ^f [10]
$E(^3A_2 \downarrow ^3A_2)$	0	0	0	0	0	0	0
$A_1(^3A_2 \downarrow ^3A_2)$	5.31	6.92	5.0734	-6.07	4.83	-1.675	-4.14
$E(^3T_2 \downarrow ^3A_1)$		7 526	7 560	7 549	7 574	7 645	7 636
$A_2(^3T_2 \downarrow ^3A_1)$	7 810	7 564	7 611	7 577	7 622	8 055	7 648
$E(^3T_2 \downarrow ^3E)$		8 392	7 704	8 500	7 948	7 687	8 036
$E(^3T_2 \downarrow ^3E)$	7 970	8 605	7 823	8 516	8 184	8 130	8 073
$A_2(^3T_2 \downarrow ^3E)$		8 828	9 173	8 757	8 306	8 287	8 228
$A_1(^3T_2 \downarrow ^3E)$		8 856	9 216	8 768	8 366	8 091	8 240
$E(^1E \downarrow ^1E)$	12 120	12 298	12 521	12 438	12 246	12 578	12 345
$A_1(^3T_1 \downarrow ^3A_2)$	12 990	13 037	12 754	13 397	12 459	12 818	13 036
$E(^3T_1 \downarrow ^3A_2)$	13 333	13 342	13 317	14 137	12 739	13 355	13 393
$A_2(^3T_1 \downarrow ^3E)$		13 630	13 050	13 792	12 974	12 999	13 273
$A_1(^3T_1 \downarrow ^3E)$	13 773	13 921	12 841	13 784	13 511	13 662	13 269
$E(^3T_1 \downarrow ^3E)$		14 196	15 627	14 143	13 849	12 661	13 822
$E(^3T_1 \downarrow ^3E)$		14 544	15 629	14 354	14 077	13 758	13 835
$A_1(^1T_2 \downarrow ^1A_1)$	19 420	19 285	20 303	20 521	19 310	19 569	20 237
$E(^1T_2 \downarrow ^1E)$	20 450	20 482	19 875	19 326	20 197	20 487	19 350
$A_1(^1A \downarrow ^1A_1)$	20 620	20 558	20 907	20 777 (20 574 ^g)	20 761	20 615	20 782
$E(^3T_1 \downarrow ^3A_2)$		21 412	22 680	21 394	21 798	21 600	21 776
$A_1(^3T_1 \downarrow ^3A_2)$	22 220	21 492	23 082	23 625	21 921	21 711	23 495
$A_2(^1T_1 \downarrow ^1A_2)$		23 643	22 881	21 437	23 666	23 616	21 832
$E(^3T_1 \downarrow ^3E)$	23 260	24 271	23 742	24 300 (24 330 ^g)	23 755	23 324	24 746
$E(^3T_1 \downarrow ^3E)$		24 345	23 329	24 255	23 827	23 618	23 746
$A_2(^3T_1 \downarrow ^3E)$		24 583	24 227	24 612 ^g	23 969	24 287	24 056
$A_1(^3T_1 \downarrow ^3E)$		24 589	24 707	25 079	24 095	24 551	24 440
$E(^1T_1 \downarrow ^1AE)$		25 035	25 337	29 431	24 431	24 484	29 712
D [8]	-5.31	-6.92	5.073 19	-6.07	-4.83	-1.675	-4.14
[40]	-5.07						
g_{\parallel} [8]	2.24	2.2879	2.246 81	2.29	2.2374	2.284	2.239
[40]	2.24 \pm 0.03						
g_{\perp} [8]	2.2	2.2225	2.252 51	2.22	2.1990	2.278	2.199
Δg [8]	0.04	0.0654	-0.005 7	0.07	0.0384	0.006	0.04

^a Calculated by substituting the spectroscopic parameters of [9], i.e. set (A), into our CDM/MSH package.

^b The results from table 1 of [9] obtained using the spectroscopic parameters in set (A).

^c The results from tables 1–3 of [10] obtained using the spectroscopic parameters in set (A).

^d Calculated by substituting the spectroscopic parameters of [8], i.e. set (B), into our CDM/MSH package.

^e The results from table 1 of [9] obtained using the spectroscopic parameters in set (B).

^f The results from tables 1 and 3 of [10] obtained using the spectroscopic parameters in set (B).

^g Disagreement between values listed in tables 1 and 2 of [10] (see text).

developed CDM approaches within the full $3d^2(3d^8)$ configuration, namely, that of [11–13], and ours, each based on a different CF scheme, strong, weak and intermediate, respectively, are free from internal errors. Consequently, the disagreement between our results and those

Table 3. Comparison between the energy levels and SH parameters calculated by Ma *et al* [11, 12] and Macfarlane [13] and the present CDM/MSH package. All values in cm^{-1} except for k and g_i . Set (C): $B = 618.4$, $Dq = 1785.4$, $C = 2502$, $\xi = 164$, $v = 879.8$, $v' = 188.5$, $k = 0.96$ [11]. Set (D): $B = 610$, $Dq = 1800$, $C = 2500$, $\xi = 155$, $v = 800$, $v' = 200$, $k = 1$ [13]. Note: we use $g_e = 2$ for a free ion in calculating the g -factors. Set (E): $B = 906$, $Dq = 829.5$, $C = 3338.0$, $\xi = 581.7$, $k = 0.81756$ [12].

		$\alpha\text{-Al}_2\text{O}_3 : \text{V}^{3+}(3d^2)$				$\text{MgO} : \text{Ni}^{2+}(3d^8)$			
Assignment C_{3v}^* ($\text{O}_h \downarrow \text{C}_{3v}$)	Expt [13]	Set (C)		Set (D)		Assignment O_h^* (O_h)	Expt [12, 42]	Set (E)	
		Ma <i>et al</i> ^a	This work ^b	Macfarlane ^c	This work ^e			Ma <i>et al</i> ^e	This work ^f
$\text{A}_1(^3\text{T}_1 \downarrow ^3\text{A}_2)$	0	0	0	0	0	$\text{T}_2(^3\text{A}_2)$	0	0	0
$\text{E}(^3\text{T}_1 \downarrow ^3\text{A}_2)$	7.85 ± 0.4 & 8.296^g	8.296	8.2960	7.9	8.0	$\text{E}(^3\text{T}_2)$	8 003	8 029	8 028.8
$\text{E}(^3\text{T}_1 \downarrow ^3\text{E})$	$810\text{--}850$ & 850^g	906.26	906.26	838	838.6	$\text{T}_1(^3\text{T}_2)$	8 179	8 179	8 178.7
$\text{E}(^3\text{T}_1 \downarrow ^3\text{E})$		1 020.35	1 020.35	946	946.2	$\text{T}_2(^3\text{T}_2)$	8 591	8 533	8 533.2
$\text{A}_2(^3\text{T}_1 \downarrow ^3\text{E})$	960	1 112.05	1 112.05	1 032	1 032.3	$\text{A}_2(^3\text{T}_2)$	8 645	8 680	8 679.6
$\text{A}_1(^3\text{T}_1 \downarrow ^3\text{E})$		1 131.10	1 131.10	1 050	1 050.6	$\text{E}(^1\text{E})$	13 100	13 072	13 072.3
$\text{E}(^1\text{T}_2 \downarrow ^1\text{E})$	8770	9 128.79	9 128.79	9 067	9 067.8	$\text{A}_1(^3\text{T}_1)$	13 120	13 110	13 109.8
$\text{E}(^1\text{E} \downarrow ^1\text{E})$	9660 & 9748 ^g	10 106.8	10 106.77	9 967	9 968.0	$\text{T}_1(^3\text{T}_1)$	13 520	13 571	13 570.7
$\text{A}_1(^1\text{T}_2 \downarrow ^1\text{A}_1)$		10 255.6	10 255.59	10 106	10 106.4	$\text{T}_2(^3\text{T}_1)$	14 333	14 290	14 290.5
$\text{A}_2(^3\text{T}_2 \downarrow ^3\text{A}_1)$		16 956.8	16 956.83	17 088	17 088.1	$\text{E}(^3\text{T}_1)$	14 770	14 800	14 799.8
$\text{E}(^3\text{T}_2 \downarrow ^3\text{A}_1)$		16 964.0	16 963.99	17 094	17 094.9	$\text{T}_2(^1\text{T}_2)$	21 126	21 140	21 140.4
$\text{A}_1(^3\text{T}_2 \downarrow ^3\text{E})$	17 420	17 347.4	17 347.45	17 444	17 444.4	$\text{A}_1(^1\text{A}_1)$		22 194	22 194.2
$\text{A}_2(^3\text{T}_2 \downarrow ^3\text{E})$		17 352.4	17 352.43	17 449	17 449.8	$\text{E}(^3\text{T}_1)$	24 552	24 583	24 583.5
$\text{E}(^3\text{T}_2 \downarrow ^3\text{E})$		17 391.9	17 391.85	17 486	17 486.5	$\text{T}_2(^3\text{T}_1)$		24 785	24 784.6
$\text{E}(^3\text{T}_2 \downarrow ^3\text{E})$	17 510	17 428.6	17 428.58	17 520	17 521.0	$\text{T}_1(^3\text{T}_1)$	25 000	24 970	24 970.3
$\text{A}_1(^1\text{A} \downarrow ^1\text{A}_1)$	21 025	20 649.7	20 649.66	20 484	20 484.1	$\text{A}_1(^3\text{T}_1)$		25 164	25 164.5
$\text{A}_1(^3\text{T}_1 \downarrow ^3\text{A}_2)$	24 930	25 000.5	25 000.54	25 020	25 020.3	$\text{T}_1(^1\text{T}_1)$	25 950	25 977	25 977.4
$\text{E}(^3\text{T}_1 \downarrow ^3\text{A}_2)$		25 014.4	25 014.43	25 034	25 034.7	$\text{E}(^1\text{E})$		32 098	32 098.3
$\text{A}_2(^3\text{T}_1 \downarrow ^3\text{E})$	25 310	25 322.9	25 322.90	25 296	25 296.9	$\text{T}_2(^1\text{T}_2)$		32 514	32 513.7
$\text{A}_1(^3\text{T}_1 \downarrow ^3\text{E})$		25 347.9	25 347.93	25 322	25 322.6	$\text{A}_1(^1\text{A}_1)$		55 527	55 526.6
$\text{E}(^3\text{T}_1 \downarrow ^3\text{E})$		25 393.7	25 393.72	25 364	25 364.6				
$\text{E}(^3\text{T}_1 \downarrow ^3\text{E})$		25 439.6	25 439.59	25 407	25 407.2				
$\text{A}_1(^1\text{T}_2 \downarrow ^1\text{A}_1)$		27 161.9	27 161.88	27 210	27 210.2				
$\text{E}(^1\text{T}_2 \downarrow ^1\text{E})$		27 557.7	27 557.68	27 584	27 584.4				

Table 3. (Continued.)

		$\alpha\text{-Al}_2\text{O}_3 : \text{V}^{3+}(3d^2)$				$\text{MgO} : \text{Ni}^{2+}(3d^8)$			
Assignment		Set (C)		Set (D)		Assignment		Set (E)	
C_{3v}^* ($O_h \downarrow C_{3v}$)	Expt [13]	Ma <i>et al</i> ^a	This work ^b	Macfarlane ^c	This work ^e	O_h^* (O_h)	Expt [12, 42]	Ma <i>et al</i> ^e	This work ^f
$A_2(^1T_1 \downarrow ^1A_2)$	29 300	29 389.4	29 389.41	29 418	29 418.0				
$E(^1T_1 \downarrow ^1E)$	30 150	29 904.9	29 904.85	29 881	29 880.7				
$A_1(^3A_2 \downarrow ^3A_2)$		35 125.77	35 125.77	35 376	35 376.3				
$E(^3A_2 \downarrow ^3A_2)$	34 500	35 125.86	35 125.86	35 376	35 376.3				
$E(^1E \downarrow ^1E)$		45 199.9	45 199.88	45 376	45 376.6				
$A_1(^1A \downarrow ^1A_1)$		57 456.7	57 456.73	—	57 525.3				
D	8.296 ± 0.016^g	8.296	8.296	7.9	7.9701	D		0	0
g_{\parallel}	1.915 ± 0.002	1.922	1.9225	1.919	1.9196	g	2.2145 ± 0.0005	2.2145	2.2145
g_{\perp}	1.74 ± 0.01	1.735	1.7346	1.719	1.7188				

^a The results from table 1 of [11] obtained using the spectroscopic parameters in set (C).

^b Calculated by substituting the spectroscopic parameters of [11], i.e. set (C), into our CDM/MSH package.

^c The results from table 1 of [13] obtained using the spectroscopic parameters in set (D).

^d Calculated by substituting the spectroscopic parameters of [13], i.e. set (D), into our CDM/MSH package.

^e The results from table 2 of [12] obtained using the spectroscopic parameters in set (E).

^f Calculated by substituting the spectroscopic parameters of [12], i.e. set (E), into our CDM/MSH package.

^g [41].

obtained by Zhou *et al* [9] and Li [10] (see table 2), as well as that reported by Li [10] regarding the results of Zhou *et al* [9], is most probably due to internal errors in either calculations of the matrix elements or the computational procedure used in [9, 10]. Hence the values of the SH parameters D , g_{\parallel} and g_{\perp} determined in [9, 10] turn out to be unreliable.

4. Summary and conclusions

We have utilized the MSH theory and developed the CFA/MSH package based on the complete diagonalization of the Hamiltonian, which includes electrostatic, CF (in the intermediate-CF scheme) and SO coupling terms. The CFA/MSH package can run under Windows and has been worked out as an extension of our previously developed CFA package. Our CFA/MSH package takes into account contributions to the SH parameters (D , g_{\parallel} and g_{\perp}) from all 45 states of $3d^8(3d^2)$ ion at trigonal (C_{3v} , D_3 , D_{3d}) symmetry sites. Hence, it enables studies of the SH parameters as functions of CF parameters Dq , v and v' . Extensive numerical calculations have been performed for several ion/host cases. We find that D and Δg ($=g_{\parallel} - g_{\perp}$) strongly depend on the trigonal CF parameter v' , whereas they are not very sensitive to the CF parameter v . The present results are used to check the accuracy of the 'quasi-fourth-order' perturbation formulae developed by PM [8], which have been widely employed by other researchers [29–32]. Our investigations show that the g -factor formulae [8] work well, especially for the cases of small v and v' and large Dq . However, the ZFS parameter D formula [8] has serious shortcomings. Our studies show that the contributions to the g -factors come mainly from the lower excited states. However, the higher excited states play an important role for the ZFS parameter D , especially in the case of Ni^{2+} ions experiencing a weaker CF in crystals (smaller Dq). Thus the contributions to the ZFS parameter from the higher excited terms cannot be neglected. Numerical calculations of the SH parameters have been performed for the Ni^{2+} and Cu^{3+} in Al_2O_3 , $LiNbO_3$ and α - $LiIO_3$ crystals. Our extensive results enable us to establish the range of validity of the PTM of PM [8] as well as to check the validity of other existing CDM approaches. It appears that the results of Zhou *et al* [9] and Li [10] are incorrect, probably due to internal errors.

Finally, let us comment on applications of the PTM and CDM to the studies of structural disorder. Since the SH parameters are very sensitive to the lattice distortions around the transition-metal ions in crystals, EPR techniques have been widely used to investigate the lattice distortions and structural disorder [33–39]. The numerical results obtained using our CFA/MSH package clearly demonstrate this feature of the SH parameters. Since our analysis shows that the PTM [8] cannot yield accurate results for some ranges of the CF parameters, the CDM should rather be adopted in the studies of the lattice distortions and structural disorder. The latter method provides accurate values of the SH parameters and thus enables extraction of information concerning the lattice distortions and structural disorder. Due to the progress in computer technology, the CDM calculations can now be easily performed on personal computers.

Recently, we have suggested [37] two lattice distortion models (I and II), in order to explain the negligible value of the ZFS parameter D , the isotropic g -factor and the large splitting $\delta(^2E)$ of the $^2E(3d^3)$ state for the double-doped $Cr^{3+} : Mg^{2+} : LiNbO_3$ crystals. The PTM results [23, 24] agree roughly with our CDM results [37] for model I, whereas there is a substantial difference between the PTM and CMD results for model II [37]. Hence the PTM cannot provide a reliable explanation for the spectroscopic features originating from the structural disorder induced by Mg^{2+} doping into these crystals. To obtain better information concerning the structural disorder and the lattice distortions one must adopt the CDM in such studies.

Acknowledgments

This work has been partially supported by a City University of Hong Kong research grant (project no 7001099) and the Education Committee Natural Science Foundation of Shanxi Province.

References

- [1] Pryce H M L 1950 *Proc. Phys. Soc. A* **63** 25
- [2] Abragam A and Bleaney B 1986 *Electron Paramagnetic Resonance of Transition Ions* (Oxford: Clarendon)
- [3] Rudowicz C 1987 *Magn. Reson. Rev.* **13** 1
Rudowicz C 1988 *Magn. Reson. Rev.* **13** 335 (erratum)
- [4] Rudowicz C and Misra S K 2001 *Appl. Spectrosc. Rev.* **36** 11
- [5] Rudowicz C and Sung H W F 2001 *Physica B* **300** 1
- [6] Blumberg W E, Eisinger J and Geschwind S 1963 *Phys. Rev.* **130** 900
- [7] Kamimura H 1962 *Phys. Rev.* **128** 1077
- [8] Petrosyan A K and Mirzakhanyan A A 1986 *Phys. Status Solidi b* **133** 315
- [9] Zhou K W, Zhao S B, Wu P F and Xie J K 1990 *Phys. Status Solidi b* **162** 193
- [10] Li Y 1995 *J. Phys.: Condens. Matter* **7** 4075
- [11] Ma D P, Ma X D, Chen J R and Liu Y Y 1997 *Phys. Rev. B* **56** 1780
- [12] Ma D P, Ma N, Ma X D and Zhang H M 1998 *J. Phys. Chem. Solids* **59** 1211
- [13] Macfarlane R M 1964 *J. Chem. Phys.* **40** 373
- [14] Yeung Y Y and Rudowicz C 1992 *Comput. Chem.* **16** 207
- [15] Yeung Y Y and Rudowicz C 1993 *J. Comput. Phys.* **109** 150
- [16] Chang Y M, Rudowicz C and Yeung Y Y 1994 *Comput. Phys.* **8** 1994
- [17] Mulak J and Gajek Z 2000 *The Effective Crystal Field Potential* (Amsterdam: Elsevier)
- [18] Newman D J and Ng B (ed) 2000 *Crystal Field Handbook* (Cambridge: Cambridge University Press)
- [19] Gerloch M and Slade R C 1973 *Ligand Field Parameters* (Cambridge: Cambridge University Press)
- [20] Wybourne B G 1965 *Spectroscopic Properties of Rare Earth* (New York: Wiley)
- [21] Morrison C A 1992 *Crystal Fields for Transition-Metal Ions in Laser Host Materials* (Berlin: Springer)
- [22] Yang Z Y 2000 *Appl. Magn. Reson.* **18** 455
- [23] Macfarlane R M 1967 *J. Chem. Phys.* **47** 2066
- [24] Macfarlane R M 1970 *Phys. Rev. B* **1** 989
- [25] Sugano S, Tanabe Y and Kamimura H 1970 *Multiplets of Transition-Metal Ions in Crystals* (New York: Academic)
- [26] Racah G 1943 *Phys. Rev.* **63** 367
- [27] Silver B L 1976 *Irreducible Tensor Methods* (New York: Academic)
- [28] Yang Z Y 2000 *Chin. J. Chem. Phys.* **13** 190
- [29] Zheng W C 1989 *Phys. Rev. B* **40** 7292
- [30] Zheng W C 1992 *Phys. Rev. B* **46** 12038
- [31] Li Z M and Li F Z 1997 *Chin. J. Chem. Phys.* **10** 20
- [32] Zheng W C 1993 *Physica B* **7** 4075
- [33] Li Z M and Shuen W L 1996 *J. Phys. Chem. Solids* **57** 1673
- [34] Yu W L 1995 *Phys. Rev. B* **52** 4237
- [35] Yang Z Y 2000 *J. Phys.: Condens. Matter* **12** 4091
- [36] Zhao M G and Xie L H 2000 *Mater. Sci. Eng. B* **74** 72
- [37] Yang Z Y, Rudowicz C and Qin J 2002 *Physica B* at press
- [38] Yamage M, Macfarlane P I, Holliday K, Henderson B, Kodama N and Inoue Y 1996 *J. Phys.: Condens. Matter* **8** 3487
- [39] Yamage M, Yosida T, Fukui M, Takeuchi H, Kodama N, Inoue Y, Henderson B, Holliday K and Macfarlane P I 1996 *J. Phys.: Condens. Matter* **8** 10633
- [40] Mirzakhanyan A A 1981 *Sov. Phys.-Solid State* **23** 1434
- [41] Pontnau J and Adde R 1975 *J. Phys. Chem. Solids* **36** 1023
- [42] Pappalarso R, Wood D L and Linares R C Jr 1961 *J. Chem. Phys.* **35** 1460
- [43] Arizmendí L, Cabrera J M and Agullo-Lopez 1984 *Ferroelectrics* **56** 79